L.R. Evans and D.J. Warner

CERN, Geneva, Switzerland

Introduction

The measurement of beam properties in proton linacs has largely been confined to the four transverse phase plane coordinates (x, x', y, y') and to the energy coordinate in the longitudinal plane. Mainly because of the experimental difficulties, the phase coordinate has not been studied in as much detail. The usefulness of measurements of beam properties via the time/phase parameter has been demonstrated in the energy spread and absolute energy measurements made at 10, 30, and 50 MeV on the PLA using a time-of-flight method.(1) However, the extension of this technique to low duty cycle injector linacs is difficult owing to the short data-collection time available.

Another approach has been developed on the CERN PS injector using a destructive coaxial probe to make real-time bunch structure measurements at 10 MeV.(2) Variants of this technique have been successfully used for 50 MeV beam studies at ANL (3) and using a sampling system at 350 keV at Saclay.(4)

The purpose of the present work was to extend the coaxial probe technique to allow us to make real-time measurements on the CERN 3 MeV experimental linac, especially in the interesting and difficult bunching region before the accelerator cavity.

Coaxial Probe Design - General Considerations

Bandwidth requirements

Consider qualitatively how the bunch length and shape vary with energy in a proton linac with an operating frequency of 200 MHz. Assuming that a pre-buncher is used, the beam will have time structure when it enters the first RF accelerating cavity with a bunch length of $\sim 60°$ (0.83 nsec). During acceleration there will be an adiabatic decrease in bunch length going approximately as $\beta^{-3/4}$. For example, with 500 keV injection the bunch lengths at 3, 10, 50, and 200 MeV would have contracted to 0.43 nsec, 0.27 nsec, 0.15 nsec, and 0.10 nsec, respectively. To measure actual bunch shapes one would require a detector bandwidth which gives a rise-time corresponding to about half the quoted times. Assuming that rise-time τ_r (nsec) and bandwidth f_b (GHz) are related by $\tau_r f_b \simeq 0.35$, one sees that even at 50 MeV the required bandwidth for good resolution is ~ 4.5 GHz, which is at the limit of present techniques in high-speed oscillography. It is therefore essential to use a matched broad-band detector in order that the oscilloscope be the limiting factor. The coaxial probe most easily fulfils this requirement.

The principle is conceptually simple -- the proton current is stopped on the inner conductor of a coaxial line and the equivalent signal is transmitted along the coaxial structure with as little attenuation as possible to be displayed on a wide-band oscilloscope.

A disadvantage of the coaxial probe is that it is destructive. However, the alternative of a transparent system as used, for example, in synchrotrons is inherently less easy to make broad-band and, more important (especially for low-energy studies), has a transit time effect which depends on its aperture.

According to the above arguments, it would seem that one requires impossibly wide bandwidths to study linac bunch shapes at high energy, but reference to the original time-of-flight work on the PLA shows that much useful information can be obtained at lower bandwidth on phase, energy, and energy spread. There is probably no alternative to a real-time broad-band system if one wishes to observe variations of beam characteristics on a bunch-to-bunch basis. Note that for measurements of a 'debunched' beam before injection into a synchrotron, bandwidths as low as 1 GHz could be sufficient.

Some possible coaxial probe geometries

In this section, general design considerations for a coaxial probe are discussed in order that solutions adopted for the 500 keV probe can be seen in perspective.

In the choice of line characteristic impedance a compromise must be reached between the allowable rise-time due to the proton transit time between inner and outer conductors, and the signal amplitude required by wide-band oscilloscopes which have inherently bad sensitivity.

For maximum vertical deflection on the oscilloscope in a perfectly matched system, one would undoubtedly choose the probe impedance to be the same as the oscilloscope (125 Ω for the Tektronix 519 used in the present work). However, transit time effects become very important for low-energy beams so that it is necessary to reduce this effect by decreasing the distance between inner and outer conductors in some way. For a given inner conductor diameter the transit time decreases with decreasing line impedance. Thus in order to maintain a good bandwidth it is necessary to reduce the impedance as much as possible.

In practice one is restricted in the choice of line impedance to those for which broad-band components are commercially available, i.e. 50 Ω, 75 Ω, and 125 Ω.

The simplest possible type of coaxial probe is an air-filled coaxial line terminated at both ends (one end by the oscilloscope) with the proton beam passing through the outer conductor with negligible energy loss and stopping on the inner conductor. With the diameter of the inner conductor determined by the aperture required (and to a lesser extent by the need to stop the beam entirely on the inner), one can readily show that the distance between inner and outer rises very quickly with impedance so that if the transit time between the outer and inner makes a significant contribution to the rise-time of the system, the lowest impedance is clearly superior. In particular, if the inner diameter is 1 cm (stopping distance in tungsten for

105 MeV protons) and the available oscilloscope bandwidth is 2 GHz (τ_r = 0.17 nsec), the transit time will be greater than τ_r below 3 MeV, 9 MeV, and 30 MeV for 35 Ω, 50 Ω, and 75 Ω lines, respectively. Evidently some modification of the ideal geometry is necessary for the coaxial probe principle to be useful at low energies with reasonable aperture.

In order to reduce the transit time while keeping the aperture and impedance constant, one could consider a number of variants of the perfectly coaxial structure. For example, the line may be distorted in some way while keeping the characteristic impedance constant, e.g. the eccentric, elliptical or strip lines shown in Fig. 1. In practice, the mechanical problems involved in matching these special line configurations to the coaxial structure for input to the oscilloscope would restrict their use only to applications where the widest bandwidth is required.

Other configurations which have been used with reasonable success are the open-ended structure used at ANL (Fig. 2) in which the protons arrive normal to the conductor cross-section, or the equivalent configuration with the beam incident through the outer conductor, as has been used at CERN. Of the two, the latter is slightly superior in that the capacitive mismatch at the end of the probe is less, and that the problem of making a wide-band elbow is obviated.

Another approach, which has been used in the present work and which alleviates the mechanical problems, is to make a localized mismatch in the probe in order to reduce the transit time. In effect, the distance between centre and outer conductor is diminished locally at the point where the beam strikes in order to reduce the transit time to an acceptable value. Obviously this introduces a capacitive mismatch which contributes to the rise-time so that the two effects have to be balanced. This approach was used for our 500 keV probe (Fig. 3).

Finally, an effect which complicates the design of coaxial probes at low energy is secondary electron emission. The proton beam impinging on the central conductor liberates slow-moving secondary electrons which may destroy the probe response. In the original probe design (2) for 10 MeV, a very convenient way of suppressing this effect was to use an air-filled probe with the protons entering via a thin aluminium window. Electrons were produced but were of low energy and were stopped by the air, whereas the energy loss of 10 MeV protons was negligible. This technique becomes impossible below about 5 MeV owing to the need to traverse a vacuum window. For pre-injector energies ($\leq$ 1 MeV) the probe must be used in vacuum so that the secondary electrons must be suppressed by some other means. In the present work the method chosen was to decouple a portion of the inner conductor from the oscilloscope by means of coaxial capacitors, and to bias it either positive or negative depending on the mode of operation.

Transmission line and oscilloscope

The two other factors which affect the system response are the oscilloscope and the attenuation in the cable between probe and oscilloscope.

Ideally the cable diameter and length should be such that the attenuation of higher harmonics is acceptable. (In all cases it should be the oscilloscope which is the limiting factor.) For example, at 2 GHz one gets 3 dB attenuation in semi air-filled coaxial cable with a length of 41 m for an outer diameter of 2.2 cm, and 17 m for an outer diameter of 1 cm.

As regards the oscilloscope, the situation has improved in the last few years, although such wide-band oscilloscopes are expensive and of limited application owing to their bad sensitivity. In the present work the oscilloscope (Tektronix 519) proved to be the main limitation on bandwidth, but was the only one available. Our restriction to real-time measurement is quite severe since present-day sampling oscilloscopes have much wider bandwidths and sensitivity.

The 500 keV Probe Design

The 500 keV probe was designed specifically for a Tektronix 519 oscilloscope (rise-time 0.29 nsec, input impedance 125 Ω). The probe characteristic impedance was chosen to be 50 ohm instead of 125 ohm owing to the transit time considerations discussed in the previous section.

The probe is shown schematically in Fig. 3. The probe head consists of a section of 50 ohm line with a 10 mm diameter inner conductor and a 23 mm diameter outer one. The head is matched to a standard GR 50 ohm rigid line by a simple taper. The vacuum seal is made by a teflon plug with viton O-rings, the inner of the line being undercut to allow for the different dielectric constant of the teflon. The other end of the head could be terminated with a coaxial GR terminating resistor or, to make full use of the available sensitivity, it could be left open circuit. Consequently the distance from the centre of the beam entry port to the open circuit was made small in order that the round-trip transit time of the reflected signal is less than the oscilloscope response.

The beam enters through a 9 mm diameter hole in the outer conductor and strikes a tungsten disc set in the inner one to eliminate the spread in transit time due to the circular cross-section of the inner conductor. The transit time across the gap between inner and outer is reduced by a tungsten grid set in the line to give a gap of only 2 mm. This inset constitutes, to a first approximation, a capacitive mismatch in the line introducing a signal rise-time RC which must be kept lower than the rise-time of the oscilloscope. With a 50 ohm load this limits the capacity to less than $\sim$ 5 pF. The effect of the capacity on the probe response is dealt with in more detail later.

In order to suppress secondary electron emission in the normal mode of operation or to accelerate electrons across the gap between inner and grid when used in the secondary emission mode, the inner conductor must be biased. Consequently a portion of the line must be capacitively decoupled from the oscilloscope and terminating resistor in such a way that the disturbance of the coaxial structure is minimal. This is achieved by cutting the inner conductor in two places and inserting into the line,

using conducting araldite, two 1 mm thick ferro-electric discs cut from a Sprague ceramic condenser. By virtue of the extremely high dielectric constant of this material, relatively high capacity can be achieved ($\sim$ 1000 pF). The thickness of the discs was chosen to withstand 2 kV bias. In order to de-couple the external circuit as effectively as pos-sible, the bias is applied through a 1 kΩ cracked carbon resistor soldered to the inner conductor and decoupled from ground by a specially made 150 pF high-frequency condenser.

Probe Operation

Normal mode

In this mode the probe records the proton current signal. To prevent secondary electron emis-sion from affecting the response, the decoupled portion of the inner was biased sufficiently posi-tive so that even taking into account the voltage swing across the 1 kΩ resistor due to the d.c. com-ponent of the incident current and the presence of the proton space charge, the bias always remained in the saturation regime for secondary electron suppres-sion. In practice, the level was determined empiri-cally as the voltage above which there was no de-tectable change in signal.

Secondary emission mode

In this mode use is made of the high second-ary emission coefficient δ of metals in this energy range ($\delta \simeq 2$ for 500 keV protons) to amplify the incident proton signal.

Protons striking the tungsten 'target' on the inner, liberate secondary electrons which must be accelerated back across the gap between inner and grid in a time which is short compared with the cir-cuit response time. The required negative bias in the absence of space charge is $\sim$ 1.2 kV to give a 0.2 nsec electron transit time. However, for large electron currents where the space-charge field be-comes important, the necessary bias may be larger. The appropriate bias point was determined empirically.

Theory

The theory given here is based on the stand-ard klystron bunching theory (without space charge).(5) In addition we develop the rudimentary extensions of the analysis so that effects which limit the fre-quency response are successively introduced by variation of the bunching parameter X across the buncher aperture, transit time between outer and inner of the probe, capacitive loading at the re-entrant insert, cable attenuation, and the oscillo-scope frequency response.

Basic bunching theory

The bunching process is described by:

$$\theta_2 = \theta_1 - X \sin \theta_1 , \qquad (1)$$

where X is a generalized bunching parameter given by

$$X = \frac{\omega \ell}{v_0} \frac{e \, V_b \, T}{m \, v_0^2}$$

with V_b the peak bunching voltage, T the transit time factor of the buncher gap, v_0 the axial (unmodulated) proton velocity, $\omega = 2\pi \times$ bunching frequency, and ℓ the bunching drift-length. In Eq. (1) $\theta_2 = \omega t_2 - (\omega \ell / v_0)$ with t_2 the time of arrival, $\theta_1 = \omega t_1$, and t_1 the time of departure of protons from the buncher.

For X < 1 there is one solution of Eq. (1) for θ_1 as a function of θ_2, whereas for X $\geq$ 1 there are three solutions of θ_1 where

$$-\left[\cos^{-1} \frac{1}{X} - (X^2 - 1)^{\frac{1}{2}}\right] < \theta_2 < \left[\cos^{-1} \frac{1}{X} - (X^2 - 1)^{\frac{1}{2}}\right] .$$
$$(2)$$

The current at the output position is given by

$$i(\theta_2) = i_0 \sum_{\theta_1(\theta_2)} \left|\frac{d\theta_1}{d\theta_2}\right| , \qquad (3)$$

where the summation is made over 1 or 3 values of θ_1 according to condition (2). Evidently this analysis gives infinities in currents when

$$\theta_2 = \pm \left[\cos^{-1} \left(\frac{1}{X}\right) - \left(X^2 - 1\right)^{\frac{1}{2}}\right] .$$

Further analysis shows that the current waveform can be analysed into harmonics, thus

$$i(\theta_2) = i_0 \left[1 + 2 \sum_{m=1}^{\infty} J_m(mX) \cos m\theta_2\right] , \qquad (4)$$

and it is the extremely slow reduction of maxima of the Bessel functions of order m, $J_m(mX)$, with m, which contribute towards the infinities found.

Radial variation of transit time factor across the buncher aperture

In a gridless buncher the parameter X varies with radius r because of the transit time factor variation:

$$X = X_0 \, I_0 \left(\frac{\omega r}{v_0}\right) . \qquad (5)$$

where I_0 is the Bessel function for imaginary argu-ment. The current at θ_2 is now given by

$$\bar{i}(\theta_2) = \frac{1}{\pi a^2} \int_0^a i(\theta_2) \, 2\pi r \, dr \qquad (6)$$

with beam radius a. It can be shown that this variation of X with r has the effect of eliminating the infinities for X > 1 but the infinity at X = 1, $\theta_1 = \theta_2 = 0$ remains. Thus the higher harmonics are less important in the waveform, and lower bandwidth is required for the detector. It should be noted that finite emittance of the beam introduces dif-ferences in path length ℓ and can be treated as if parameter X changes for different regions of trans-verse phase space.

Effect of transit time in the probe

Assume that a proton crossing the gap from outer to inner in a coaxial probe represents a con-stant current during the transit time τ_f. One can represent this folding by

$$\bar{i}(\theta_2, \tau_f) = \frac{1}{\tau_f} \int_{(\theta_2/\omega)-(\tau_f/2)}^{(\theta_2/\omega)+(\tau_f/2)} \bar{i}(\theta_2) \, dt_2 \ . \qquad (7)$$

Expressing $\bar{i}$ as a Fourier series:

$$\bar{i} = a_0 + \sum_{1}^{\infty} a_n \cos n\theta_2 \ , \qquad (8)$$

and making the integration (7) we find the modified Fourier components

$$a_n(\tau_f) = a_n(0) \ \sin\left(\frac{n\omega\tau_f}{2}\right) \Big/ \left(\frac{n\omega\tau_f}{2}\right) \qquad (9)$$

which is a familiar ideal transit time factor.

Effect of capacitive loading

Assume that a mismatched insert in the line at the beam aperture forms a shunting capacity across an ideal line terminated at each end by its characteristic impedance R_0. The response of the probe to current described by $\bar{i}(\theta_2)$ will be

$$V(\theta_2) = \bar{i}(\theta_2) \ Z(\omega) \ , \qquad (10)$$

so that the coefficients of the series are modified by the factor

$$\frac{2|Z(\omega)|}{R_0} = \left[1 + (n\omega \ CR_0/2)^2 \right]^{-\frac{1}{2}} \qquad (11)$$

and in the phase term, $\cos (n\theta_2 + \phi)$,

$$\phi = -\tan^{-1} (n\omega \ CR_0/2) \ . \qquad (12)$$

For an open circuit line $R_0/2$ is replaced by R_0 in Eqs. (11) and (12).

Effect of cable attenuation

The r.f. cable between probe and oscilloscope will produce a frequency dependent attenuation composed of two terms, one due to conductor losses, the other due to dielectric losses:

$$\alpha(n) = \alpha_c \sqrt{n} + \alpha_d n \qquad (13)$$

with constants α_c and α_d derived from published cable attenuation data at (for example) 200 MHz and 2 GHz. Thus, after ℓ metres of cable the nth harmonic will be reduced by a factor:

$$F(n) = \exp \left[-\alpha(n)\ell \right] \qquad (14)$$

Oscilloscope response

The quoted response of the oscilloscope is given as a rise-time τ_r. Assume that the bandwidth corresponding to τ_r is the 3 dB point on frequency response characteristic and that frequency response varies like the transit time factor of elements of the deflecting line in the travelling wave tube. Ignoring any phase distortion effects, we quote the frequency response as

$$T(n) = \frac{\sin \left[(n\omega \ \tau_s)/2 \right]}{(n\omega \ \tau_s)/2} \ , \qquad (15)$$

where characteristic time τ_s is defined by the 3 dB point.

Computed results

A computer program was written to calculate firstly the basic bunched current waveform as given by Eq. (3), then the successive filtering processes were applied. While the signal $i_2(\theta)$ still contains infinities or very high harmonics (n > 20), we use the full signal [Eq. (3)], i.e. we do not analyse into harmonic components. After filtering has been applied in such a way as to reduce one of the higher harmonics to zero (e.g. transit time effect in the probe), then the results are calculated via Eq. (4). Results obtained via Eq. (3) are plotted for five values of X in Fig. 4. To show the effect of each successive filtering process we take as an example $X_0 = 2.0$, and compare in Fig. 5 the waveforms obtained: a) from Eq. (3); b) after allowing variation of X across the buncher aperture; c) with (b) and after putting in filtering due to finite transit time in the probe; d) with (b) and (c) plus effect of capacitive loading; e) with (b), (c), and (d) plus the effect of the cable attenuation; f) with effects (b) to (e) inclusive and the oscilloscope response. A set of waveforms was calculated for comparison with the experimental results; these are given in Fig. 6.

One important effect which we have not taken into account in the present analysis is the influence of space charge. In the 3 MeV linac one would expect this to make an extremely important contribution to the bunch shape, since the currents in the low-energy drift space are large (300 → 500 mA).

Experimental Results

Several of the novel features of the coaxial probe were specifically applicable to measurements with a bunched 500 keV proton beam, in particular the use of secondary electron emission to increase the probe sensitivity. In addition, the rise-time of the available oscilloscope ($\tau_r = 0.29$ nsec) was sufficiently good to show interesting detail at 500 keV, whereas by 3 MeV the phase damping has in theory reduced the bunch length by a further factor of 2.

The layout of the low-energy drift space of the 3 MeV accelerator is given in another paper at this conference(6). The coaxial probe is placed where there is normally a set of variable apertures (BA2) so that in fact the bunching distance is reduced from 820 mm (to the middle of the first cell) to ∿ 650 mm. This reduction has a more drastic effect on the beam focusing via triplet T2 than on the longitudinal bunching itself.

During the first experiments we found difficulty in holding the bias on the inner of the probe. This was interpreted as being due to arcing induced by the beam producing very high instantaneous temperatures on the tungsten inset thereby liberating adsorbed gas and even electrode material. Fortunately this effect had a time constant of a few microseconds, so that by working just after the leading edge of the proton pulse it was possible to obtain reproducible results. Initial experiments comparing the open

ended with the terminated arrangement showed no detectable difference in bunch form except for the factor of two increase in signal amplitude. This would suggest that the stray capacity caused by the re-entrant grid is not the major limitation of the rise-time. To study this specific point we would have found it advantageous to use a lower loss cable as the present one gave $\sim$ 4 dB attenuation at 2 GHz.

The results presented here are specifically to show the operation of the probe rather than its use in proton dynamics studies. They show a) the effect of buncher voltage on bunch shapes, b) the effect of space charge, and c) the use of the probe in the secondary emission mode.

One expects from the theoretical treatment that since the peak buncher voltage is proportional to the parameter X, the characteristic shapes ranging from unbunched to over-bunched should be observed.

In Fig. 6 this effect is shown for a beam current at the buncher of 200 mA and with the probe biased at +1 kV for electron suppression. For comparison some calculated waveforms are shown with the values of X and beam radius a chosen to match best at maximum buncher level. The beam radius was increased from 8.5 mm to 10 mm but the other attenuation parameters were unchanged from their actual nominal values.

To show the effect of space charge, the current into the buncher was varied by changing the triplet T1 and taking as the mean current in the buncher-probe space that measured on BM3. The results given in Fig. 7, taken over a range of values of buncher voltage, show, as expected, that the onset of the characteristic over-bunching waveform occurs at higher buncher voltage as the nominal current is increased from 100 mA to 400 mA.

The third experiment involved the use of negative bias to amplify the signal via the secondary electrons emitted from the inner of the probe. Figure 8 shows some typical signals as a function of bias. It can be seen that although the frequency response seems to be slightly worse in the secondary emission mode, it is still sufficiently good to resolve the double bunch structure.

In previous papers we have stressed the effect which back-streaming secondary electrons can have on a beam under measurement. Although one might expect less of a perturbation when the beam is bunched (as the trapping potential well is not constant in time and space), one should not ignore it in dynamics studies. The simplest technique for eliminating back-streaming secondary electrons would be to use a positively biased aperture before the probe.

Conclusions

The feasibility of real time proton bunch measurements at 500 keV has been demonstrated. There are some obvious areas where improvements could be made particularly in the bandwidth of the detection system and in suppression of arcing. In the secondary emission mode the coaxial probe gave encouraging results and showed that the reduction in bandwidth was acceptable. The coaxial probe technique has now been used successfully at 500 keV, 10 MeV and 50 MeV but at the higher energies the bandwidth required was too high for phase spread measurements. However a possible region where lower bandwidth could be acceptable is after the debunching of a proton beam and before injection into a synchrotron.

REFERENCES

1) K. Batchelor, A. Carne, J.M. Dickson, D.J. Warner, Beam Energy Measurements on the Rutherford Laboratory PLA, Proc. 1964 Linear Accelerator Conference (MURA), p. 372.

2) D.J. Warner, An Approach to 200 MHz Bunch Measurements, Proc. 5th Int. Conf. on High Energy Accelerators, Frascati (1965), p. 612.

3) R. Perry, J. Abraham, Measurements of Phase Shift due to Beam Loading in an Alvarez-Type Linac, Proc. 6th Int. Conf. on High Energy Accelerators, Cambridge (1967), p. 270.

4) P. Bernard et al., New 20 MeV Saturne Injector Studies on Ion Sources and Particles Bunching, Proc. 6th Int. Conf. on High Energy Accelerators, Cambridge (1967), p. A8.

5) D.R. Hamilton, J.K. Knipp, J.B.H. Kuper, Klystrons and Microwave Triodes (McGraw-Hill, 1948), p. 202.

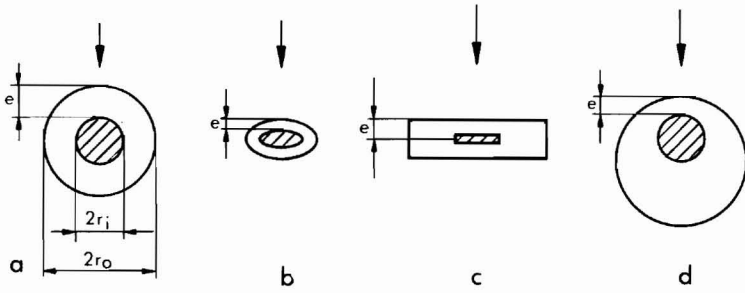6) D.J. Warner, Accelerator Research and Development with the CERN 3 MeV Linac, This Conference.

Fig. 1 : 50 Ω lines (a) Normal, (b) Elliptical,
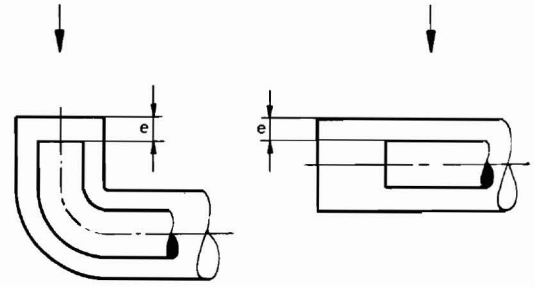(c) Strip , (d) Eccentric

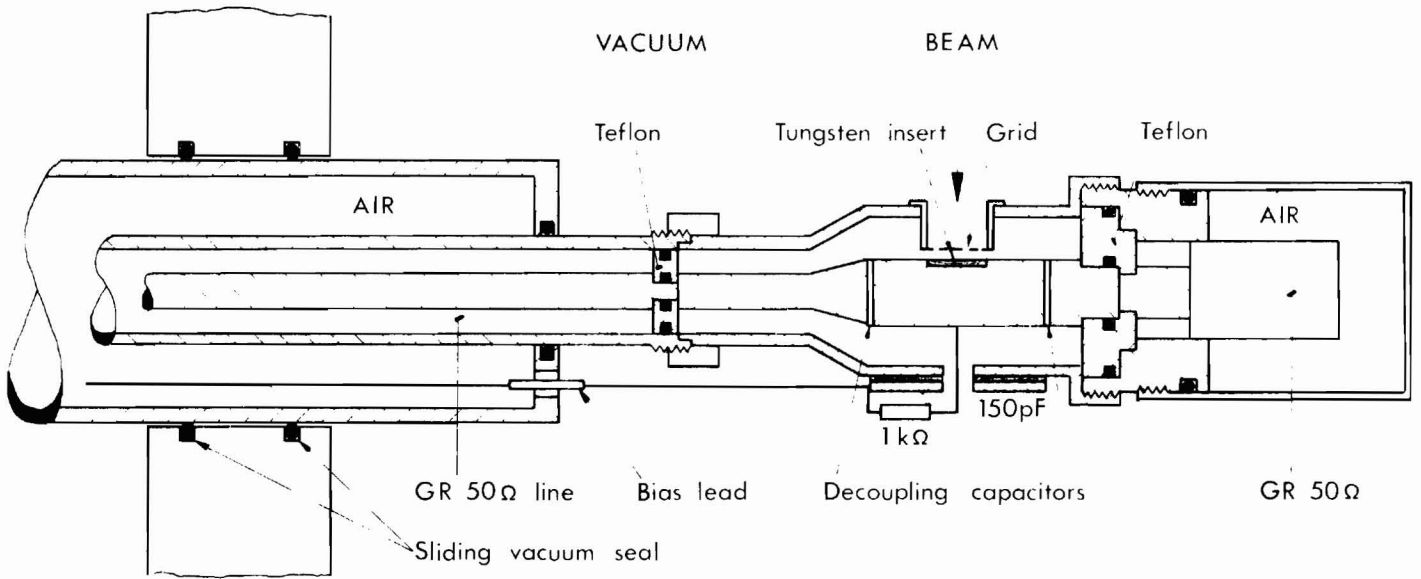Fig. 2 . Open Circuit Probes (a) End Entry
(b) Side Entry

VACUUM   BEAM

Teflon   Tungsten insert   Grid   Teflon

AIR   AIR

150pF

1 kΩ

GR 50Ω line   Bias lead   Decoupling capacitors   GR 50Ω

Sliding vacuum seal

Fig. 3   Coaxial Probe used with 500 keV beam

Fig. 4   Ideal Bunch Form for X_o = 0.0(0.5) 2.5

X_o = 2.0
a = 8.5 mm
τ_f = 0.3 nS
C = 5 pF
R_o = 50 Ω
α_c = 0.103/m
α_d = 0.018/m
τ_g = 0.37 nS

a
b
c
d
e
f
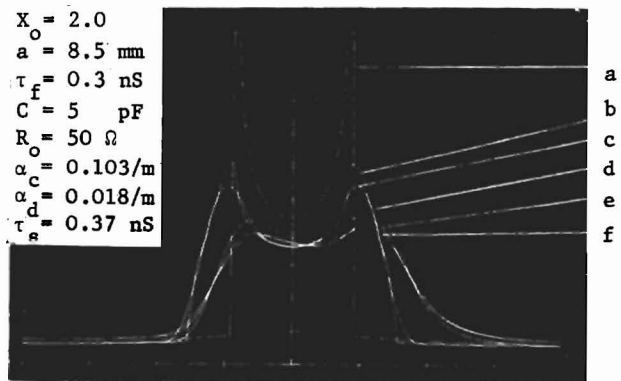
Fig. 5   Waveforms with Successive Attenuations

$X_o = 2.0$
1.8
1.6
1.4
1.2
1.0
0.8
0.6
0.4

(a)   (b)
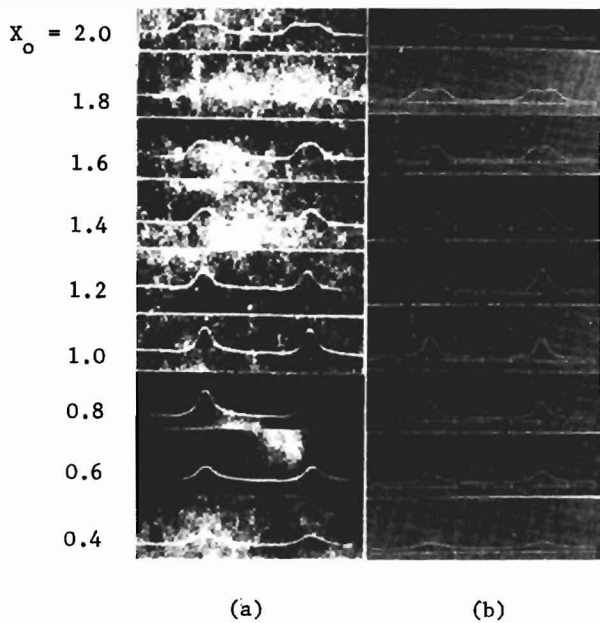
Fig. 6   Comparison of Experiment (a) and Theory (b)

Bias = – 2   kV
– 1.5 kV
– 1.0 kV
– 0.5 kV
– 0.0 kV
+ 0.5 kV
+ 1.0 kV
+ 1.5 kV
+ 2.0 kV

Fig. 3   Effect of Bias on Overbunched Signal

$X_o = 2.2$
2.0
1.8
1.6
1.4
1.2
1.0
0.8
0.6
0.4

I = 100 mA   I = 200 mA   I = 300 mA   I = 400 mA
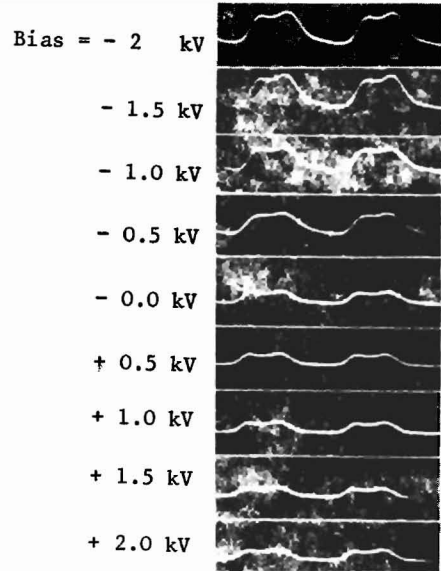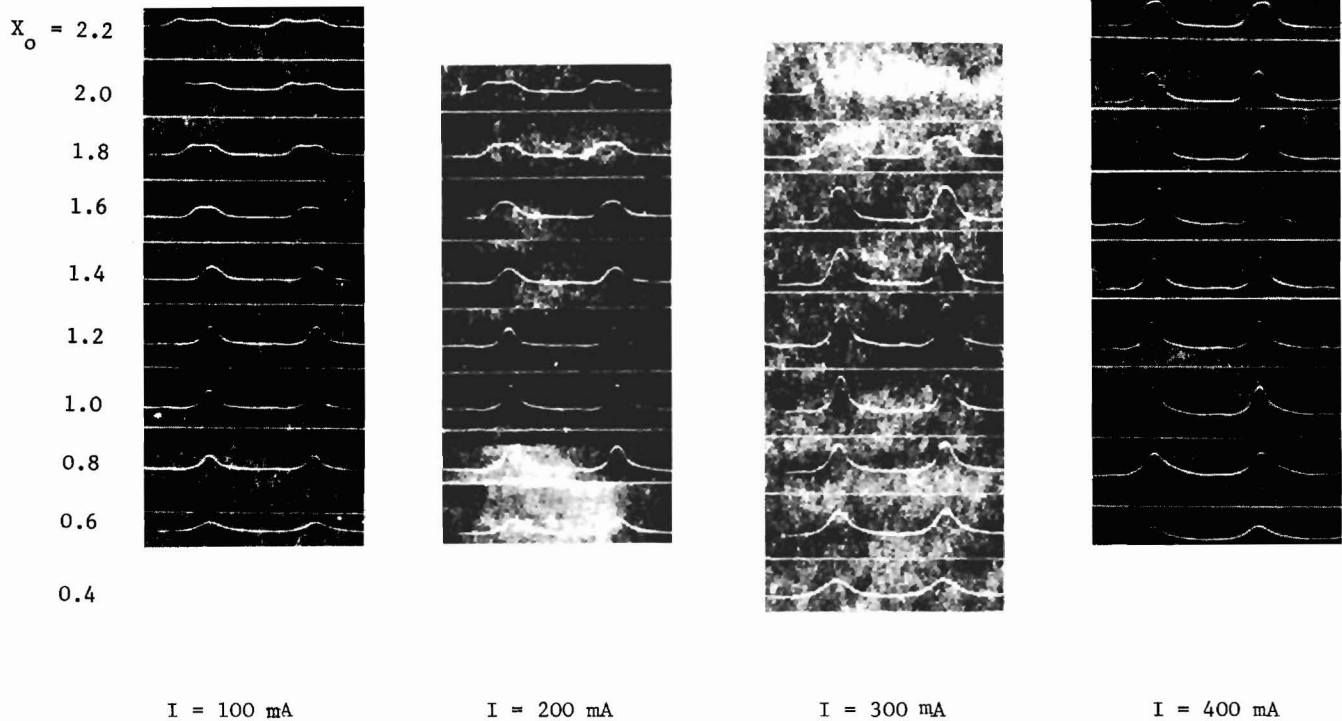
Fig. 7   Variation of Measured Waveforms with Current